Nanoscale

PAPER

View Article Online
View Journal | View Issue



Cite this: *Nanoscale*, 2019, **11**, 6755

# Films of filled single-wall carbon nanotubes as a new material for high-performance air-sustainable transparent conductive electrodes operating in a wide spectral range

A. A. Tonkikh, *[a,b] V. I. Tsebro,[c,d] E. A. Obraztsova,[a,e] D. V. Rybkovskiy,[f,a] A. S. Orekhov,[g,h] I. I. Kondrashov,[a] E. I. Kauppinen,[i] A. L. Chuvilin[j,k] and E. D. Obraztsova[a,b]

Received 19th December 2018,
Accepted 4th March 2019

DOI: 10.1039/c8nr10238d

rsc.li/nanoscale

In this paper we show the advantages of transparent high conductive films based on filled single-wall carbon nanotubes. The nanotubes with internal channels filled with acceptor molecules (copper chloride or iodine) form networks demonstrating significantly improved characteristics. Due to the charge transfer between the nanotubes and filler, the doped-nanotube films exhibit a drop in electrical sheet resistance of an order of magnitude together with a noticeable increase of film transparency in the visible and near-infrared spectral range. The thermoelectric power measurements show a significant improvement of air-stability of the nanotube network in the course of the filling procedure. For the nanotube films with an initial transparency of 87% at 514 nm and electrical sheet resistance of 862 Ohm sq$^{-1}$ we observed an improvement of transparency up to 91% and a decrease of sheet resistance down to 98 Ohm sq$^{-1}$. The combination of the nanotube synthesis technique and molecules for encapsulation has been optimized for applications in optoelectronics.



## Introduction

Single-wall carbon nanotubes (SWCNTs) show a unique set of physical and chemical properties such as high mobility of charge carriers,[1] ballistic transport along the nanotube axis,[2] chemical stability,[3] *etc*. However, these properties are inherent only to the individual SWCNTs. In general, for different applications, such as transparent conductive films (TCF) or light sensitive structures in electronic devices, the SWCNTs are merged in macrostructures as films,[4] fibers[5] and mats.[6] It is quite natural that nano-objects assembled in macrostructures lose or change their characteristics. For instance, the high conductivity (up to 30 000 S cm$^{-1}$ (ref. 7 and 8)) and mobility (up to 100 000 cm$^2$ V$^{-1}$ s$^{-1}$) decrease by several orders of magnitude in assembled nanotubes.[9,10]

This happens because the mixture of as-synthesized non-treated SWCNTs usually contains both metallic and semiconducting nanotubes,[11] and the SWCNTs by themselves are not well-aligned and not perfectly straight.[12–16] Moreover, there is a significantly high contact resistance between individual SWCNTs or between their bundles when they are collected in films, wires or mats.[17–20] Because of these features, the as-synthesized SWCNTs assembled in transparent conductive films (TCF) are inferior to the widely used materials such as indium–tin oxide (ITO), PEDOT:PSS, Ag-nanowires or FTO/ITO electrodes which have an $R_{sq}$ of 20–30 Ohm sq$^{-1}$ under the same optical transmission $T_{tr}$.[21–23]

There are several ways to enhance the conductivity of the as-synthesized SWCNT films: a post-synthesis treatment of SWCNTs (like chemical doping, an attachment of functional

[a]*A.M. Prokhorov General Physics Institute, RAS, 38 Vavilov Street, 119991 Moscow, Russia. E-mail: aatonkikh@gmail.com*
[b]*Moscow Institute of Physics and Technology, 9 Institutskiy per., 141701 Dolgoprudny, Moscow Region, Russia*
[c]*P.N. Lebedev Physical Institute, RAS, 53 Leninsky Prospect, 119991 Moscow, Russia*
[d]*Kapitza Institute for Physical Problems, RAS, 2 Kosygina Street, 119334 Moscow, Russia*
[e]*Shemyakin and Ovchinnikov Institute of Bioorganic Chemistry, RAS, 16/10 Miklukho-Maklaya Street, 117871 Moscow, Russia*
[f]*Skolkovo Institute of Science and Technology, Skolkovo Innovation Center, 143026, 3 Nobel Street, Moscow, Russia*
[g]*Shubnikov Institute of Crystallography of FSRC "Crystallography and Photonics" RAS, 119333 Moscow, Russia*
[h]*Electron Microscopy for Materials Science (EMAT), University of Antwerp, 2020 Antwerpen, Belgium*
[i]*Depart. of Applied Physics, Aalto University, School of Science, P.O. Box 15100, FI-00076 Espoo, Finland*
[j]*CIC nanoGUNE Consolider, Tolosa Hiribidea 76, 20018 Donostia-San Sebastian, Spain*
[k]*IKERBASQUE Basque Foundation for Science, Maria Diaz de Haro 3, E-48013 Bilbao, Spain*

groups to the CNT walls, *etc*.[24–28]); a post-synthesis separation of the SWCNT mixture into metallic and semiconductor fractions;[29] an alignment and densification of SWCNTs in films to decrease the number of contacts and to shorten the electric current path;[30] a selective growth of SWCNTs with a preferential conductivity type.[31] These approaches allow the increase of the conductance of SWCNT films by an order of magnitude.

Also, in addition to the conductive properties of TCF, the operating spectral range and the methods of deposition and formation are important. This is primarily due to the utilization of transparent conductive electrodes in solar cells (organic), transparent displays, LEDs, OLEDs and photosensitive detectors.[32–34] In such typically layered structures, it is necessary to have a transparent top electrode. According to modern requirements and depending on the specific application, the top electrode should have a high conductivity, transparency in the operating range, flexibility, stability, low toxicity, low cost, and embeddability in the manufacturing process.[35] Unfortunately, there is no universal material for TCF. ITO, despite its high conductivity and transparency, is a fragile material, with a narrow window of transparency (visible range) and a high cost.[32,36] Moreover, the methods of CVD growth and sputtering of ITO are not applicable to the formation of organic solar cells, light-sensitive elements, and OLEDs.[37] PEDOT, PEDOT:PSS, Ag nanowires, acid-doped CNTs and externally doped CNTs are superior to ITO in many ways, but the main problem is the formation and deposition of such electrodes.[32,33,35,38] The formation process of organic electrodes involves the use of suspensions with surfactants and solvents, drop-casting deposition and doping on an already formed structure of LEDs or solar cells.[17,18,39] Such treatments contaminate or destroy the layered structures.

In the present work we show the advantages of gas phase filling of the SWCNT interior channels by acceptor molecules (which is usually utilized for synthesis of unique 1D-structures[25,40–42] in the context of TCF production). This method is very promising due to the higher stability of such films in comparison with the films assembled from SWCNTs with functionalised outer walls.[27,43–45] We have found efficient parameters for SWCNT conductivity improvement through encapsulation. For nanotube synthesis and film formation we used the aerosol-CVD synthesis where the SWCNT film is automatically formed at the bottom of the chamber.[46] We used gas-phase filling of SWCNTs by copper chloride or iodine.[24,47–49] Our previous articles demonstrate a significant change in optical and electrical properties of single- and multiwall CNTs after encapsulation of copper chloride or iodine. In our approach we have selected these dopants due to a high encapsulation efficiency, an ability of filling from the gaseous phase and a substantial charge transfer between dopant and nanotube. From our point of view, this approach is the most versatile and satisfies all requirements for the top electrode. The optimized filling technique and the method of nanotube synthesis make it possible to deposit films that are already doped. A high conductivity and a wide transparency range make this material promising as multipurpose transparent conductive films (TCF).

In this paper, we investigated the conductivity and thermoelectric power (TEP) as a function of temperature for "pristine", iodine- and copper chloride-doped SWCNT films to estimate the advantages and the features of TCF based on filled SWCNTs. Also, the optical transmission ($T_{tr}$) improvements of a unique set of aerosol-grown SWCNT films with $T_{tr}$ = 60–90% were discovered. The effect of different charge transfer on optical and electrical properties of films was investigated. The most important practical results are the complex improvement of TCF based on filled-SWCNTs. The increase of transparency within a very wide spectral range, the increase of conductivity by an order of magnitude and the presence of environmental insensitivity and flexibility were discovered for our samples.

## Experimental

### Preparation of SWCNT network and sample description

In this work the aerosol chemical vapor deposition (CVD) prepared SWCNTs were used for the formation of transparent conductive flexible electrodes. The aerosol-SWCNTs are synthesized in vertical laminar flow reactors. The experimental setups for aerosol synthesis include a precursor feed system, a furnace with a metal or ceramic tube and sampling and analysis devices.[46] The advantages of aerosol CVD synthesis are:

- formation of extended SWCNT films consisting of relatively long (more than 1 μm) nanotubes and their bundles;
- growth of SWCNTs with large diameters (up to 2 nm);
- possibility of assembling SWCNTs in transparent highly conductive flexible buckypaper structures;
- possibility of tuning gradually several parameters: the SWCNT diameters, buckypaper density and optical transparency.

These features make aerosol-SWCNTs very promising for the formation of transparent conductive flexible electrodes. The films synthesized by aerosol CVD are networks formed from long bundles of SWCNTs. The nanotubes have a mean diameter of 1.8 nm (Fig. 1(b)). For our investigation the SWCNT films were prepared with transparency ($T_{tr}$) in the range from 60 to 90% (Fig. 1(a)). The nanotube network transparency was controlled by changing the time of accumulation

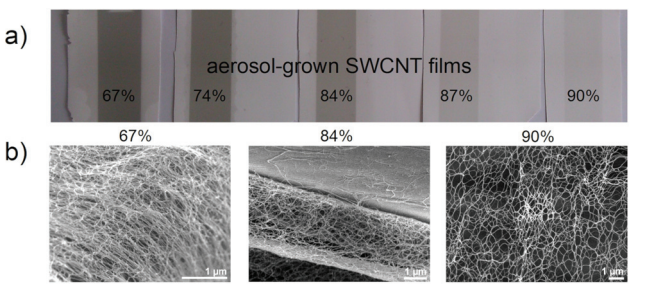


Fig. 1 (a) Photograph of a set of aerosol-grown SWCNT films with different optical transparencies (transparency values are given for 514 nm); (b) SEM images of aerosol-grown SWCNT films with different optical densities.

of SWCNTs on the filter (Millipore, pore size of about 0.45 nm) during synthesis. Initial $R_{sq}$ of prepared films was in the range from 150 Ohm $sq^{-1}$ to 4800 Ohm $sq^{-1}$ depending on $T_{tr}$, with higher resistance for higher transparency. For instance, the films with $T_{tr}$ of 67% and 87% showed an $R_{sq}$ of 150 and 860 Ohm $sq^{-1}$, respectively. As it was noted in the Introduction, the main disadvantages affecting the conductivity of films based on assembled nanotubes are high electrical resistance of contacts between the nanotube bundles and relatively low concentration of metallic (conductive) nanotubes in the SWCNT mixture. In this work we apply a new approach to increase the electrical conductivity of semiconducting SWCNTs in films. It is based on gas-phase filling of the nanotubes with copper chloride or iodine. From each sample shown in Fig. 1(a) (samples with transparency 60–90%) 3 strips have been cut for studies. A comparison of doping effects was performed with those strips of each sample.

### The doping procedure of the SWCNT network

A simple method of SWCNT doping was used. The SWCNT films were deposited on polished quartz plates and heated at 200 °C in air for 2 hours to remove organics. At the main stage of the treatment procedure a sealed tube with the sample and doping crystals was heated up in an electric furnace. There were no direct contacts between the nanotube network and the crystals.[24] The treatment temperature should be close to the sublimation temperature of the dopant materials. The sublimation temperature value of crystalline iodine is 113.5 °C. The iodine treatment was carried out in the temperature range of 125–130 °C[49] over 14 hours. About 20 mg of solid iodine (Sigma-Aldrich, 99.8%) was used for the treatment process.

The second dopant used for the same SWCNT films was copper chloride. According to the literature, copper chloride demonstrated a higher, in comparison with iodine, charge transfer value, while the treatment procedure was also quite simple.[47,48] A gas-phase treatment by copper chloride was carried out in the temperature range of 210–230 °C for 26 hours. We used 1–5 mg of solid copper(I) chloride (Alfa Aesar, metals basis, 99.999%) for treatment.

A post-treatment procedure includes heating of treated films in an un-sealed tube for 2 hours under the same treatment conditions but without dopant crystals. This step was performed to partly remove the outer-wall adsorbed dopant crystals. A doping effect due to nanotube filling and other changes in the nanotube film properties were compared in the case of iodine and copper chloride treatment.

### Optical, microscopic and transport measurements of prepared materials

The Raman spectra of "pristine", iodine- or copper chloride-treated SWCNT films were obtained with a Jobin Yvon S-3000 spectrometer and an Ar–Kr laser (Spectra-Physics). The Raman spectra of SWNTs were recorded with 514 nm (2.41 eV) excitation wavelength in the spectral ranges of tangential G-mode (around 1600 $cm^{-1}$) and radial breathing modes (RBM) (50–500 $cm^{-1}$). The UV-vis-NIR optical absorption spectra were recorded within a spectral range of 200–3000 nm with a Lambda-950 spectrophotometer (PerkinElmer).

The measurements of electrical resistance of aerosol-synthesized SWCNT films were made by an ordinary DC four-probe method, using the Keithley 220 model as the switchable current source, and the Keithley 182 model for measuring the potential drop. The measured current was $10^{-7}$ A. The films were fixed in a special holder. Contacts to the sample were manufactured from a 30 μm diameter copper wire and attached with a self-solidifying silver paste. In our investigations we measured not only the value of the electrical resistance at room temperature but also its temperature dependence in the range of 5 to 300 K. For this purpose the holder was placed in a blown-through helium cryostat for intermediate temperatures.

The thermoelectric power (TEP) was measured using an ordinary integral two-probe method[50] in a specialized vacuum chamber containing a custom-made TEP probe holder. On gradient heating the holder plate the sample temperatures and the potential differences across the sample are measured with thermocouples. The chromel–alumel thermocouples were utilized as probes, but the potential differences were measured by alumel wires. The samples of "pristine", iodine- and copper chloride-filled SWCNT films were held under the ambient conditions before the TEP measurements. The measurements were conducted for a temperature range of 300–425 K (temperature of the hot point of the sample) and in air.

The treated SWCNT films were studied by scanning electron microscopy (SEM) using a JEOL-7600F instrument and by high resolution transmission electron microscopy (HRTEM) using the instrument JEM-2100F equipped with a delta corrector and a cold field emission gun operated at 60 kV.

TEM studies should reveal the filling of interior channels of SWCNTs after gaseous treatment of both types. For iodine we have already observed this earlier.[24] As was shown, the gaseous treatment leads to the filling of nanotube channels and the formation of one-dimensional (1D) structures inside. In the case of iodine the 1D crystals or polyiodide chains were observed depending on the diameters of SWCNTs.[49] In our work we used the coarse aerosol-grown SWCNTs with a mean diameter of 1.8 nm (Fig. 2(a) shows an example of a "pristine" nanotube). In our case only 1D crystals were observed inside nanotubes after iodine or copper chloride treatment (Fig. 2(b) and (c)). The atomic structure of 1D-crystals of iodine and copper halides, formed within carbon nanotubes with diameters up to ~1.6 nm, has been studied in numerous experimental and theoretical studies.[51–55] In relatively thin nanotubes, the filling molecules may arrange in unique 1D-structures, and not exist as free-standing objects. For large-diameter tubes it is often believed that the filled material resembles the structure of the corresponding bulk crystal. However, recent studies revealed an unexpected complexity of the 1D nanocrystals grown inside the nanotube's inner channels.[56] Treatment of the CNT-samples with binary compounds may result in the growth of different substances with various chemical compo-

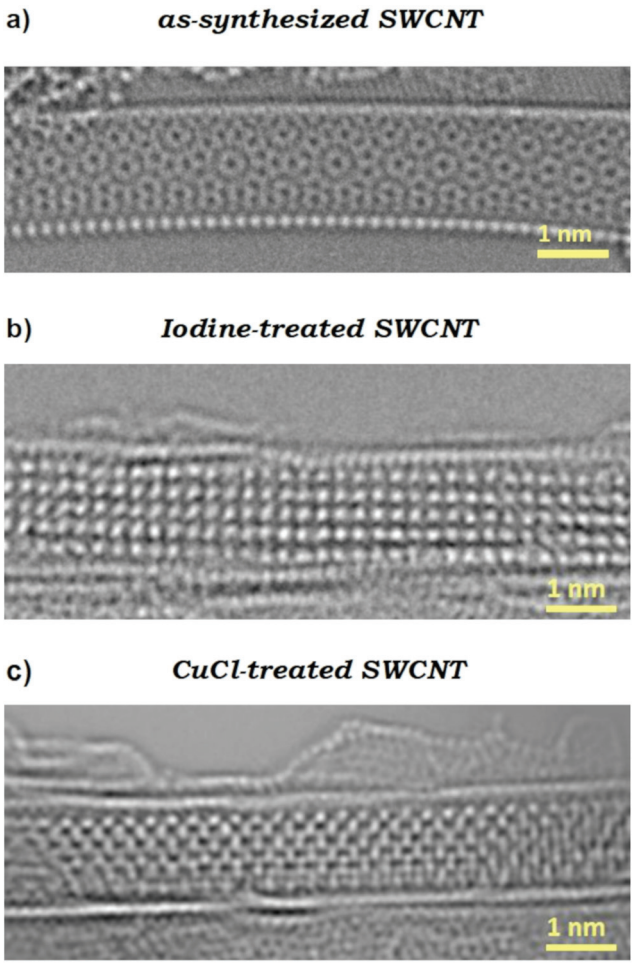


Fig. 2 HRTEM images of (a) initial SWCNTs; (b) SWCNTs filled with iodine; (c) SWCNTs filled with CuCl.

sitions. An unambiguous determination of the chemical composition and precise atomic arrangement of the 1D-crystals grown inside the carbon nanotubes requires a more detailed study including theoretical modeling and analysis of different TEM projections.

## Results and discussion

Many properties of carbon nanotubes are affected by chemical doping. Due to a large difference between the work function values of carbon nanotubes (~4.95–5.05 eV (ref. 57 and 58)) and strong acceptor solids like iodine (~5.5 eV (ref. 59)) and copper chloride (~6.8–7.0 eV (ref. 60)), the electrons from the CNTs are transferred to the lower-lying states of the acceptor structures. The consequence of this charge transfer is the depletion of the highest occupied nanotube electronic states and Fermi level shift inside the valence band of the CNTs,[25,53] which leads to metallization of the semiconducting fraction of the macroscopic sample. Besides the enlarged electrical conductivity,[47,61,62] this also significantly affects the optical properties of the samples – the Burstein–Moss shift,[63,64] observed in degenerate semiconductors, manifests itself in the suppression of optical absorption bands of the nanotubes.[49,65,66] In the context of transparent conductive film fabrication, the acceptor doping leads, therefore, to the overall improvement of the SWCNT film characteristics, making them both more conductive and more transparent. We now turn to the detailed discussion of the properties of the produced films, probed by optical absorption, thermoelectric and conductivity measurements.

### Raman and UV-vis-NIR spectra

The Raman spectra of pristine and gas-phase treated SWCNT films were recorded at 514 nm (2.41 eV) excitation wavelength (Fig. 3). The normalized Raman spectra of treated SWCNTs show a significant change in the phonon and electron structure of SWCNTs. In the case of iodine, the G-band was shifted toward high frequencies by 2–3 $cm^{-1}$. The right shift of the G-band was associated with the charge transfer from SWCNTs to dopant structures.[67–69] In the low frequency range a significant suppression of radial breathing mode (RBM) bands and an appearance of a new line were detected.[70] The suppression of SWCNT modes could be associated both with a charge transfer and a strong mechanical interaction between nanotubes and 1D structure inside them. Some contribution could come from dopant clusters outside the tube walls. As was reported,[49] the new peaks in the RBM region are lines of polyiodide structures, formed inside nanotube inner channels and, probably, in the space between individual tubes in bundles. Moreover, because the $I_2$ lines were not discovered in the spectra, we could conclude that adsorbed or intercalated $I_2$ is absent.[49]

The Raman spectra of copper chloride-treated SWCNTs exhibited similar effects. In the case of copper chloride, the significant suppression of RBM, 2D and G bands was observed.[48] As well as in the case of iodine the right shift of the G-band associated with charge transfer was detected. As

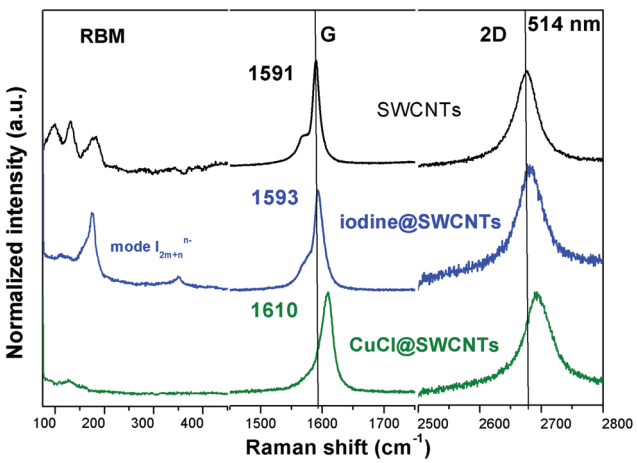


Fig. 3 The normalized Raman spectra of SWCNT films formed from initial and acceptor-filled (iodine or CuCl) nanotubes. The excitation wavelength is 514 nm (2.41 eV).

was expected, the shift was higher than that in the case of iodine by an order of magnitude (up to 20 $cm^{-1}$) as a consequence of higher charge transfer in the case of copper chloride.

UV-vis-NIR spectra (in spectral range 200–3000 nm) were recorded for SWCNT films of different densities, and, as a result, of different optical transparencies. Fig. 4(a) shows the optical features of "pristine" SWCNTs. The bands marked as E11s, E22s and E11m are associated with electron transitions for semiconducting (s) and metallic (m) SWCNTs, respectively. It was determined that the measured samples (60–90% transparency) demonstrated $T_{tr}$ of 67, 74, 84, 87% and 90% at 514 nm, depending on film density.

After gas-phase iodine treatment the changes in optical properties triggered by the charge transfer from SWCNTs to iodine structures were observed (Fig. 4(b)). The first electron transition for semiconducting SWCNTs was completely suppressed. The second electron transition for semiconducting SWCNTs was suppressed partially. The suppression of electron transition occurs due to the charge transfer which empties the states in the top of the valence band. In these states there are no electrons which could absorb photons anymore. The suppression of E11s and E22s is related to the position of the Fermi energy and allows the estimation of the efficiency of electron transfer from the nanotube. Another effect is a decrease of $T_{tr}$ in spectral region 200–1500 nm. A reduction of transparency (of 3% in average) was observed for all samples at 514 nm (Fig. 4(b)). The increase of absorption in the entire visible range may be attributed to the absorption of 1D polyiodide structures, formed inside the nanotubes.[71]

Fig. 4(c) presents the UV-vis-NIR spectra of copper chloride-treated SWCNTs. As in the case of iodination, the electron transitions for semiconducting SWCNTs were also suppressed. However, for copper chloride the suppression effect was higher. This correlates with the Raman results for both cases (Fig. 3). Thus, for copper chloride a higher value of charge transfer was observed, as in the previous studies.[47,49,53] As for the optical transparency, the opposite effect takes place. The samples with initial $T_{tr}$ of 67%, 74% and 84% at 514 nm were not remarkably affected, while for the samples with initial $T_{tr}$ of 87% and 90% the increase of $T_{tr}$ of about 4% was detected. In the case of copper chloride, the effect of transparency increase, resulting from the charge transfer, was observed up to the ultraviolet range, where copper chloride absorbs. After the copper chloride treatment a new band appeared in the UV region at the position of about 360 nm. We attribute this band to the absorption of a chlorine-containing substance.[72] Also, the position of the observed band is close to that known for nano-objects of CuCl and $CuCl_2$.[73,74]

Improving the transparency and expanding the spectral transparency window is one of the significant advantages of filled-SWCNTs compared to the widely-used TCF materials. This work and our recent[75] investigations show that the film of filled SWCNTs is highly transparent within a wide range – from 200 up to 10 000 nm. The organic materials (as PEDOT:PSS) have a narrow transparent spectral window (from 300 up to 1000 nm).[76] Also, the ITO and FTO/ITO structures are trans-

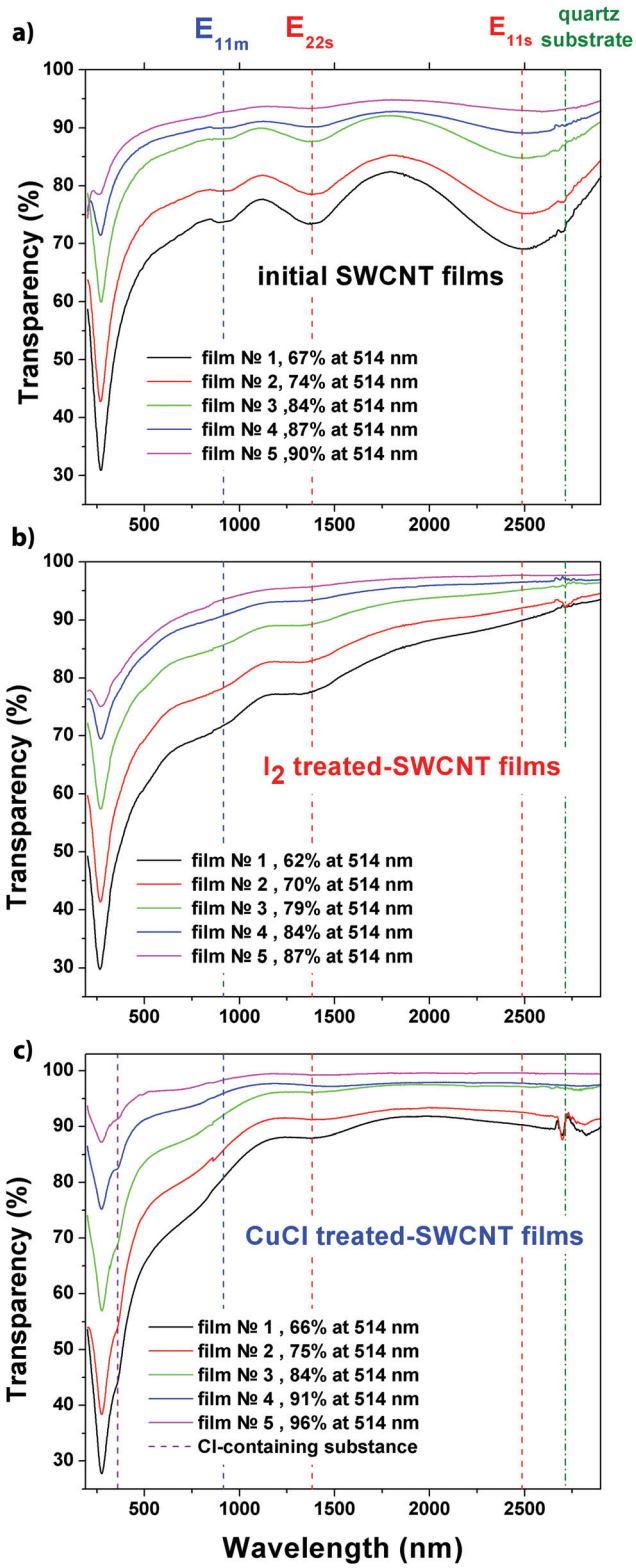


Fig. 4 UV-vis-NIR optical absorption spectra for the set of SWCNT films with different optical transparencies (film no. 1–5): (a) initial; (b) filled with iodine; (c) filled with CuCl.

parent within the visible range, but they have an extremely high light absorption in UV and NIR ranges.[77]

### Stability of doped SWCNT films

The stability of single-walled carbon nanotube films filled with CuCl and iodine was estimated by thermoelectric power (TEP) measurements. TEP is extremely sensitive to the Fermi energy shift. Moreover, for semiconductors, the TEP sign yields the type of predominant carrier as well as the value of energy gap.

The plots of Fig. 5 demonstrate the measured TEP (Seebeck coefficient) as a function of average temperature for initial, iodine- and copper chloride-doped SWCNT films. Here all measurements were made in the narrow temperature range from 298 to 373 K and under air conditions for 20 minutes. The Seebeck coefficient of initial SWCNT films shows the exponential change from about +120 μV $K^{-1}$ to −7 μV $K^{-1}$ at slight heating. Such behavior is easily explained by the extreme sensitivity of the SWCNT's electronic properties to the presence of physisorbed or/and chemisorbed oxygen.[78,79] Oxygen is known to show acceptor properties for carbon nanotubes. So in our case, the physical desorption of oxygen, caused by heating, leads to the change of carrier type from holes to electrons with a switching of the Seebeck coefficient sign – TEP signs are switching from plus to minus.

Despite the fact that physisorbed oxygen is present in the copper chloride and iodine treated samples, the TEP temperature-induced behavior of initial and intentionally doped samples was significantly different. The TEP of copper chloride and iodine-doped SWCNT films showed a weak dependence on the temperature within the whole range. Such temperature dependence is usual for metallic SWCNTs.[80] Presumably, the effect of oxygen desorption for a filled-SWCNT film is negligible. Primarily, it is due to a strong doping and a significant Fermi level shift for iodine (0.6 eV) and copper chloride (0.9 eV) doped samples.[47]

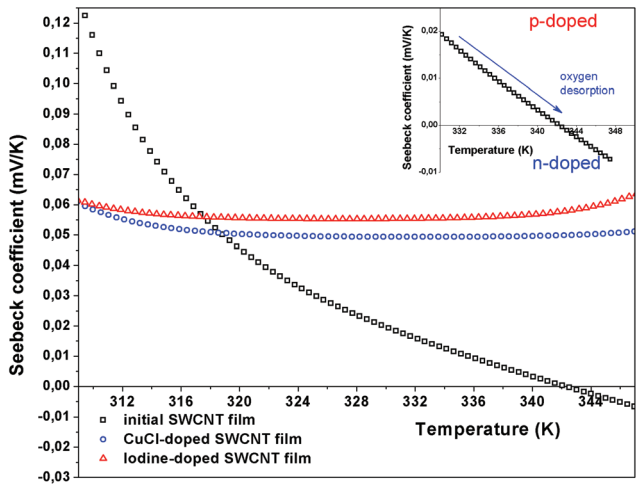


Fig. 5 Temperature dependence of thermopower for initial, iodine- and CuCl-doped SWCNT films. Insertion: Thermopower for initial SWCNT films in the region of TEP sign switching.

Based on the TEP results we show that under the filling process the SWCNT films become more air-sustainable. In this case, stability depends on evaporation temperature and doping ability of fillers. The initial samples are doped by physisorbed oxygen, so heating above 300 K leads to its desorption having a negative effect on transport properties: an increase in the resistance is triggered by the change in the carrier type. The filling (physisorption) with iodine and copper chloride was carried out at 403 and 503 K, respectively. Thus, the intentionally doped films demonstrate the stable transport properties below 400 K. In the case of simultaneous physisorption of a few acceptors (or donors), the main contribution to the transport properties is determined by the strongest one. It happens due to the highest carrier density under the stronger doping effect. The additional oxygen doping leads to a minor change in carrier density. Therefore iodine- and copper chloride-doped samples are stable within the temperature range investigated. Such insensitivity to the environment makes the filled tubes a very promising material for electronics applications.

### Sheet resistance of doped SWCNT films

Four-probe DC measurements were carried out at room temperature for the untreated, iodine-treated and copper chloride-treated SWCNTs assembled in films of different optical transparencies. To investigate the improvement of film electrical conductivity after the gas-phase treatment by iodine or copper chloride, the strips of samples with 60–90% transparency were placed on quartz substrates and connected by a 30 μm-diameter copper wire, attached with a self-solidifying silver paste. As was expected, a high charge transfer led to a remarkable improvement of electrical conductive properties of filled SWCNT films. Previously, we and other groups observed a substantial increase in the film electrical conductivity, triggered by the charge transfer between the nanotube and dopant.[24,47,62]

The 4-probe measurements have demonstrated an extremely high decrease of $R_{sq}$ for both iodine- and copper chloride-treated SWCNT films. For example, for the least transparent initial sample, the iodine treatment changed the values of $R_{sq}$ from 147 Ohm to 31 Ohm and $T_{tr}$ from 67% to 62%. The same "pristine" film after the copper chloride treatment demonstrates $R_{sq}$ and $T_{tr}$ of 28 Ohm and 66%. So, the improvement of $R_{sq}$ by an order of magnitude was observed in both cases. On the other hand, in the case of initially more transparent films the difference between the nanotube filling with copper chloride and iodine is clearly detected. The film with an initial $R_{sq}$ and $T_{tr}$ of 4800 Ohm and 90% after the iodine treatment changed to 359 Ohm and 87% and after the copper chloride treatment – 208 Ohm and 96% (Table 1). In comparison with the iodine treatment, the copper chloride filling led to a higher (about two-fold) decrease of $R_{sq}$. The higher effect on $R_{sq}$ of SWCNT films in the case of copper chloride treatment could be assigned to the higher value of charge transfer in this case, confirmed earlier by the Raman and UV-vis-IR studies of the same films. The difference in the $R_{sq}$ and $T_{tr}$ changes for different SWCNT films may be

 

**Table 1** The electrical sheet resistance ($R_{sq}$) at room temperature and optical transparency ($T_{tr}$) at 514 nm for initial and filled SWCNT films

| SWCNT films | | Iodine-treated SWCNT films | | Copper chloride-treated SWCNT films | |
|---|---|---|---|---|---|
| $T_{tr}$ (%) | $R_{sq}$ (Ohm) | $T_{tr}$ (%) | $R_{sq}$ (Ohm) | $T_{tr}$ (%) | $R_{sq}$ (Ohm) |
| 67 | 147 | 62 | 31 | 66 | 28 |
| 74 | 261 | 70 | 61 | 75 | 31 |
| 84 | 362 | 79 | 68 | 84 | 60 |
| 87 | 862 | 84 | 151 | 91 | 98 |
| 90 | 4807 | 90 | 359 | 96 | 208 |

explained by the features of filling degree and percolation effects. With the increase of film density (toward lower $T_{tr}$) the number of metal current pathways should increase. Thus the effect of SWCNT film doping should be lower for high density films containing both metal and semiconducting tubes.

From the point of view of transparent conductive films the most important results concern the samples with initial coupling of parameters $T_{tr}|R_{sq}$ of 84%|362 Ohm as well as 87%|862 Ohm. Iodine doping of these samples led to a change of $T_{tr}|R_{sq}$ from 79%|68 Ohm to 84%|151 Ohm. The copper chloride doping of these samples led to these characteristics changing to 84%|60 Ohm and 91%|98 Ohm, respectively. Thus, the highest parameter of $T_{tr}|R_{sq}$ at the transparency closest to 90% has been observed for SWCNT films treated with copper chloride. This film demonstrated $T_{tr}|R_{sq}$ characteristics close to those of ITO. Moreover, these new films formed from assembled doped SWCNTs turned out to be very stable. As was specially tested, their $T_{tr}$ and corresponding $R_{sq}$ values remain unchanged for several years. The control measurements of sheet resistance at room temperature have been performed in a few years. The SWCNT films, treated with copper chloride, with 84 and 91% transparency, demonstrated an increase in sheet resistance from 60 to 63 Ohms and from 98 to 102 Ohms, respectively. So, the variation of resistance did not exceed 6% after five years.

The temperature dependencies of the sheet resistance of the investigated SWCNT films are shown in Fig. 6. As seen, all the curves have a non-monotonic temperature dependence with a strongly pronounced metallic behavior ($dR/dT > 0$) at high temperatures and an abrupt up-turn at low temperatures. It is also seen that a weak metallic behavior at $T > 200$ K is observed even for "pristine" SWCNT films. However, as was mentioned by us in ref. 24, such a behavior appears to be observed only for the films consisting of SWCNTs with an average diameter equal or greater than 2 nm. For the films made from SWCNTs of lower average diameter the up-turn $R(T)$ began directly from room temperature.

After modification by doping, the film resistance appeared to drop down by one order of magnitude, to change the non-monotonic temperature behavior, and to reduce the crossover temperature. The greatest effect is observed in the case of using copper chloride as a dopant. The metallic behavior of $R(T)$ is extended down to 50 K.

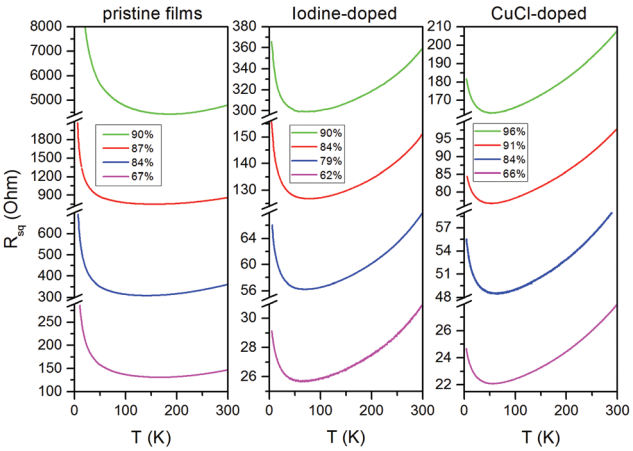


**Fig. 6** Temperature dependencies of the sheet resistance of pristine and doped SWCNT films with different values of optical transparency.

As follows from the data shown in ref. 47, the forms of reduced $R(T)/R(300\ K)$ dependencies almost do not depend on optical transparency, *i.e.* on the density of nanotube cells in the nanotube net. In turn, this fact argues a presence of two contributions to the total resistance: (1) the contribution from SWCNT bundles with a quasi-one-dimensional conductivity; (2) the contribution from the inter-bundle electron tunneling in the place of their crossing. As was shown in ref. 47 these contributions are perfectly fitted in frames of the known heterogeneous model.[81,82] The modification of SWCNTs by doping decreases the values of both contributions. The behavior of nanotube contribution can be described in frames of the model for suppression of backscattering of the charge carriers by phonons. The shift of the Fermi energy from the gap center into the valence band was determined in ref. 47 as −0.6 eV in the case of iodine doping and as −0.9 eV in the case of copper chloride doping. It was also shown that in the case of SWCNT film modification the energy barriers for electron tunneling between SWCNT bundles are essentially diminished. This means that there is a significant decrease of contact resistance between SWCNT bundles. In addition, the dropping down of the energy barriers for electron tunneling by one order of magnitude substantially exceeds the decreasing of nanotube contribution specified by a low energy phonon participation.

Thus, from a physical point of view the significant decrease of the electrical resistance of acceptor-doped SWCNTs assembled into transparent films can be connected with the shift of the Fermi level down into the valence band in the region of quasi-one-dimensional density of states. The level of doping corresponding to the Fermi energy shift below the top of the first metallic sub-band provides the increase of conductivity of metallic nanotubes, and simultaneously, the opening of a metallic channel for p type doped semiconducting nanotubes. Thereto it is very important that the doping leads to the significant decrease of the energy barriers for electron tunneling between SWCNT bundles, and therefore to essential diminishing of the contact resistance between SWCNT bundles.

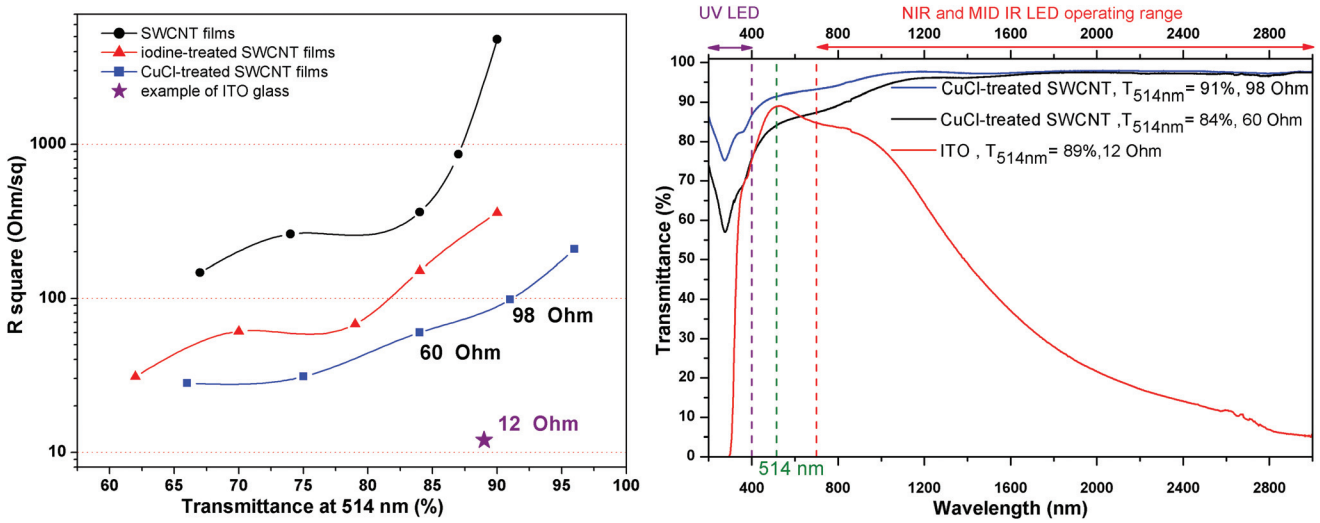


Fig. 7 (Left) The electrical sheet resistance ($R_{sq}$) at room temperature *versus* optical transparency ($T_{tr}$) at 514 nm for films assembled from pristine and filled SWCNTs. (Right) UV-vis-NIR optical absorption spectra for ITO glass and copper chloride-doped films.

### Advantages of filled SWCNT films

The discussed changes in the conductive and optical properties of SWCNT films arising after acceptor-doping are summarized in Fig. 7. The SWCNT films treated with copper chloride demonstrate the lowest sheet resistance, which is, however, 5–8 times higher than that of the ITO glass sample used for comparison. The ITO glass with a transparency of 89% at a wavelength of 514 nm and a sheet resistance of 12 Ohm was used as a reference sample. These values are better than the ones observed for the filled nanotube films. Nevertheless such films are still promising for the formation of conductive transparent electrodes. The final resistance of the transparent doped nanotube film is strongly dependent on the initial parameters of the sample before doping. We believe that by optimizing the methods of synthesis and film formation it is possible to achieve much lower values of resistance of initial samples. As a result, a minimal resistance of these films after treatment with copper chloride will be decreased. In general, such films demonstrate significant advantages compared with ITO and other organic and nanotube transparent electrodes. They have a higher transparency in the wide spectral range from 200 to 10 000 nm. This makes it possible to use such films for UV, IR and MID IR LEDs, as well as other photosensitive elements where it is necessary to make a transparent conductive "window"[83–88] From our point of view, the other most important advantage of such films is a possibility of their simple non-disturbing incorporation into many technological processes for the formation of layered structures (especially organic ones). Such ability exists due to the simplicity of transferring aerosol CVD grown films on any surface without additional thermal treatment, participation of solvents and organic materials.[4,89] Also the filling technique can be optimized for doping of free-standing films anywhere with the subsequent transfer to the formed layered structure. This eliminates the contamination of photosensitive layered elements and the destruction of fragile organic structures. Another equally important advantage is a temporary stability and insensitivity to the environment, even in the course of longstanding temperature processes. According to the thermoelectric measurements, the filled carbon nanotubes are almost not sensitive to the absorption and desorption of oxygen. Moreover, a long-standing storage in air (5 years) leads to an electrical resistance increase of no more than 6%.

## Conclusions

In the present work we demonstrate the advantages of networks of single-wall carbon nanotubes filled with acceptor molecules (iodine, copper chloride) from the gas phase. The gaseous treatment results in the encapsulation of iodine or copper chloride into SWCNT channels, followed by the formation of 1D-structures based on them. These 1D-structures accept electrons from the nanotubes. We have revealed the effective charge transfer between the nanotubes and inner structures. This led to the remarkable improvement of characteristics of "pristine" conductive SWCNT networks: sheet resistance, wide-range optical transparency and air sustainability. The higher charge transfer leads to the higher improvement of electrical sheet resistance of the film formed from hybrid (nanotube + dopant) structures. Thus, the copper chloride encapsulation improves the $R_{sq}$ of the aerosol-synthesized SWCNT films more than the iodine treatment. A unique set of conductive films with a step-by-step changed transmission (60–95%) has been prepared in this work on the basis of aerosol-synthesized single-wall carbon nanotubes. The nanotubes were filled with iodine or copper chloride under the same conditions. The effect of transparency and sheet resis-

 

tance improvement in films of filled nanotubes (compared with parent pristine ones) was observed for all films in the set. The highest couples of values of $T_{tr}|R_{sq}$ – 84%|60 Ohm and 91%|98 Ohm have been registered. These characteristics sound very promising for applications in optoelectronics. Thus, the filling procedure is not only a method for increasing conductivity. We demonstrate that filling is a comprehensive method of improving transparency, conductivity, and stability of nanotube networks for use as conductive transparent flexible electrodes in optoelectronic devices operating in ultraviolet, visible and infrared spectral ranges in different environments.

## Conflicts of interest

There are no conflicts to declare.

## Acknowledgements

The work was supported by the RFBR project 18-29-19113-mk, grant no. 311533 of Academy of Finland, Russian Federation President Program for young scientist MK-3140.2018.2. Also, the reported study was funded by RFBR and Moscow city Government according to the research project no. 19-32-70004. TEM measurements were performed with financial support from the Ministry of Science and Higher Education of the Russian Federation within the state assignment for the Federal Scientific Research Centre "Crystallography and Photonics" of the Russian Academy of Sciences.



## Notes and references

1 T. Dürkop, S. A. Getty, E. Cobas and M. S. Fuhrer, *Nano Lett.*, 2004, **4**, 35–39.
2 M. Biercuk, S. Ilani, C. Marcus and P. L. McEuen, in *Carbon Nanotubes, Topics in Appl. Phys.*, 2007, vol. 111, pp. 455–493.
3 D. Y. Khang, J. Xiao, C. Kocabas, S. MacLaren, T. Banks, H. Jiang, Y. Y. Huango and J. A. Rogers, *Nano Lett.*, 2008, **8**, 124–130.
4 O. Reynaud, A. G. Nasibulin, A. S. Anisimov, I. V. Anoshkin, H. Jiang and E. I. Kauppinen, *Chem. Eng. J.*, 2014, **255**, 134–140.
5 B. Vigolo, *Science*, 2000, **290**, 1331–1334.
6 D. Suppiger, S. Busato and P. Ermanni, *Carbon*, 2008, **46**, 1085–1090.
7 A. Thess, R. Lee, P. Nikolaev, H. Dai, P. Petit, J. Robert, C. Xu, Y. H. Lee, S. G. Kim, A. G. Rinzler, D. T. Colbert, G. E. Scuseria, D. Tomanek, J. E. Fischer and R. E. Smalley, *Science*, 1996, **273**, 483–487.
8 R. H. Baughman, *Science*, 2002, **297**, 787–792.
9 I.-W. Peter Chen, R. Liang, H. Zhao, B. Wang and C. Zhang, *Nanotechnology*, 2011, **22**, 485708.
10 W. Zhou, W. Ma, Z. Niu, L. Song and S. Xie, *Chin. Sci. Bull.*, 2012, **57**, 205–224.
11 R. Saito, M. Fujita, G. Dresselhaus and M. S. Dresselhaus, *Appl. Phys. Lett.*, 1992, **60**, 2204–2206.
12 H. Zhao, Y. Zhang, P. D. Bradford, Q. Zhou, Q. Jia, F.-G. Yuan and Y. Zhu, *Nanotechnology*, 2010, **21**, 305502.
13 J. Hicks, A. Behnam and A. Ural, *Phys. Rev. E: Stat., Nonlinear, Soft Matter Phys.*, 2009, **79**, 012102.
14 G. Cunningham, M. Lotya, N. McEvoy, G. S. Duesberg, P. van der Schoot and J. N. Coleman, *Nanoscale*, 2012, **4**, 6260.
15 T. Drwenski, S. Dussi, M. Dijkstra, R. van Roij and P. van der Schoot, *J. Chem. Phys.*, 2017, **147**, 224904.
16 A. V. Kyrylyuk, M. C. Hermant, T. Schilling, B. Klumperman, C. E. Koning and P. van der Schoot, *Nat. Nanotechnol.*, 2011, **6**, 364–369.
17 D. Zhang, K. Ryu, X. Liu, E. Polikarpov, J. Ly, M. E. Tompson and C. Zhou, *Nano Lett.*, 2006, **6**, 1880–1886.
18 F. Mirri, A. W. K. Ma, T. T. Hsu, N. Behabtu, S. L. Eichmann, C. C. Young, D. E. Tsentalovich and M. Pasquali, *ACS Nano*, 2012, **6**, 9737–9744.
19 Z. Z. Wu, *Science*, 2004, **305**, 1273–1276.
20 A. Buldum and J. P. Lu, *Phys. Rev. B: Condens. Matter Mater. Phys.*, 2001, **63**, 161403.
21 S. Kim, S. Y. Kim, M. H. Chung, J. Kim and J. H. Kim, *J. Mater. Chem. C*, 2015, **3**, 5859–5868.
22 K. Sun, P. Li, Y. Xia, J. Chang and J. Ouyang, *ACS Appl. Mater. Interfaces*, 2015, **7**, 15314–15320.
23 W. W. He, X. H. Yan, Y. F. Long, Y. M. Liang, C. Pan, J. L. Zhao and Q. X. Liu, *IOP Conf. Ser. Mater. Sci. Eng.*, 2017, **242**, 012006.
24 A. A. Tonkikh, V. I. Tsebro, E. A. Obraztsova, K. Suenaga, H. Kataura, A. G. Nasibulin, E. I. Kauppinen and E. D. Obraztsova, *Carbon*, 2015, **94**, 768–774.
25 A. Eliseev, L. Yashina, M. Kharlamova and N. Kiselev, in *Electronic Properties of Carbon Nanotubes*, InTech, 2011.
26 S. Niyogi, M. A. Hamon, H. Hu, B. Zhao, P. Bhowmik, R. Sen, M. E. Itkis and R. C. Haddon, *Acc. Chem. Res.*, 2002, **35**, 1105–1113.
27 H.-Z. Geng, K. K. Kim, K. P. So, Y. S. Lee, Y. Chang and Y. H. Lee, *J. Am. Chem. Soc.*, 2007, **129**, 7758–7759.
28 J. E. Fischer, *Acc. Chem. Res.*, 2002, **35**, 1079–1086.
29 C. Y. Khripin, A. Fagan and M. Zheng, *J. Am. Chem. Soc.*, 2013, **135**, 6822–6825.
30 M. C. LeMieux, M. Roberts, S. Barman, Y. W. Jin, J. M. Kim and Z. Bao, *Science*, 2008, **321**, 101–104.
31 J. R. Sanchez-Valencia, T. Dienel, O. Gröning, I. Shorubalko, A. Mueller, M. Jansen, K. Amsharov, P. Ruffieux and R. Fasel, *Nature*, 2014, **512**, 61–64.
32 W. Cao, J. Li, H. Chen and J. Xue, *J. Photonics Energy*, 2014, **4**, 040990.
33 Y. Zhou, H. Cheun, S. Choi, C. Fuentes-Hernandez and B. Kippelen, *Org. Electron.*, 2011, **12**, 827–831.
34 F. Qin, J. Tong, R. Ge, B. Luo, F. Jiang, T. Liu, Y. Jiang, Z. Xu, L. Mao, W. Meng, S. Xiong, Z. Li, L. Li and Y. Zhou, *J. Mater. Chem. A*, 2016, **4**, 14017–14024.

35 M. Kaltenbrunner, M. S. White, E. D. Głowacki, T. Sekitani, T. Someya, N. S. Sariciftci and S. Bauer, *Nat. Commun.*, 2012, **3**, 770.
36 N. Kim, H.-D. Um, I. Choi, K.-H. Kim and K. Seo, *ACS Appl. Mater. Interfaces*, 2016, **8**, 11412–11417.
37 D. S. Hecht, L. Hu and G. Irvin, *Adv. Mater.*, 2011, **23**, 1482–1513.
38 E.-X. Ding, Q. Zhang, N. Wei, A. T. Khan and E. I. Kauppinen, *R. Soc. Open Sci.*, 2018, **5**, 180392.
39 A. Iyer, A. Kaskela, L.-S. Johansson, X. Liu, E. I. Kauppinen and J. Koskinen, *J. Appl. Phys.*, 2015, **117**, 225302.
40 J. T. Ye, Z. K. Tang and G. G. Siu, *Appl. Phys. Lett.*, 2006, **88**, 1–4.
41 K. Hirahara, K. Suenaga, S. Bandow, H. Kato, T. Okazaki, H. Shinohara and S. Iijima, *Phys. Rev. Lett.*, 2000, **85**, 5384–5387.
42 A. I. Chernov, P. V. Fedotov, H. E. Lim, Y. Miyata, Z. Liu, K. Sato, K. Suenaga, H. Shinohara and E. D. Obraztsova, *Nanoscale*, 2018, **10**, 2936–2943.
43 Y. Zhou and R. Azumi, *Sci. Technol. Adv. Mater.*, 2016, **17**, 493–516.
44 R. Jackson, B. Domercq, R. Jain, B. Kippelen and S. Graham, *Adv. Funct. Mater.*, 2008, **18**, 2548–2554.
45 H. Peng, L. B. Alemany, J. L. Margrave and V. N. Khabashesku, *J. Am. Chem. Soc.*, 2003, **125**, 15174–15182.
46 A. Moisala, A. G. Nasibulin, D. P. Brown, H. Jiang, L. Khriachtchev and E. I. Kauppinen, *Chem. Eng. Sci.*, 2006, **61**, 4393–4402.
47 V. I. Tsebro, A. A. Tonkikh, D. V. Rybkovskiy, E. A. Obraztsova, E. I. Kauppinen and E. D. Obraztsova, *Phys. Rev. B*, 2016, **94**, 245438.
48 P. V. Fedotov, A. A. Tonkikh, E. A. Obraztsova, A. G. Nasibulin, E. I. Kauppinen, A. L. Chuvilin and E. D. Obraztsova, *Phys. Status Solidi*, 2014, **251**, 2466–2470.
49 A. A. Tonkikh, E. A. Obraztsova, E. D. Obraztsova, A. V. Belkin and A. S. Pozharov, *Phys. Status Solidi*, 2012, **249**, 2454–2459.
50 A. T. Burkov, A. Heinrich, P. P. Konstantinov, T. Nakama and K. Yagasaki, *Meas. Sci. Technol.*, 2001, **12**, 264–272.
51 X. Fan, E. C. Dickey, P. C. Eklund, K. A. Williams, L. Grigorian, R. Buczko, S. T. Pantelides and S. J. Pennycook, *Phys. Rev. Lett.*, 2000, **84**, 4621–4624.
52 L. Guan, K. Suenaga, Z. Shi, Z. Gu and S. Iijima, *Nano Lett.*, 2007, **7**, 1532–1535.
53 A. A. Eliseev, L. V. Yashina, N. I. Verbitskiy, M. M. Brzhezinskaya, M. V. Kharlamova, M. V. Chernysheva, A. V. Lukashin, N. A. Kiselev, A. S. Kumskov, B. Freitag, A. V. Generalov, A. S. Vinogradov, Y. V. Zubavichus, E. Kleimenov and M. Nachtegaal, *Carbon*, 2012, **50**, 4021–4039.
54 N. A. Kiselev, R. M. Zakalyukin, O. M. Zhigalina, N. Grobert, A. S. Kumskov, Y. V. Grigoriev, M. V. Chernysheva, A. A. Eliseev, A. V. Krestinin, Y. D. Tretyakov, B. Freitag and J. L. Hutchison, *J. Microsc.*, 2008, **232**, 335–342.
55 D. V. Rybkovskiy, A. Impellizzeri, E. D. Obraztsova and C. P. Ewels, *Carbon*, 2019, **142**, 123–130.
56 C. Nie, A.-M. Galibert, B. Soula, L. Datas, J. Sloan, E. Flahaut and M. Monthioux, in *2016 IEEE Nanotechnology Materials and Devices Conference (NMDC)*, IEEE, 2016, pp. 1–2.
57 M. Shiraishi and M. Ata, *Carbon*, 2001, **39**, 1913–1917.
58 A. A. Zhukov, V. K. Gartman, D. N. Borisenko, M. V. Chernysheva and A. A. Eliseev, *J. Exp. Theor. Phys.*, 2009, **109**, 307–313.
59 H. Yamamoto, K. Seki, T. Mori and H. Inokuchi, *J. Chem. Phys.*, 1987, **86**, 1775–1779.
60 A. Goldmann and D. Westphal, *J. Phys. C: Solid State Phys.*, 1983, **16**, 1335–1343.
61 R. S. S. Lee, H. J. J. Kim, J. E. E. Fischer, A. Thess and R. E. E. Smalley, *Nature*, 1997, **388**, 255–257.
62 Y. Zhao, J. Wei, R. Vajtai, P. M. Ajayan and E. V. Barrera, *Sci. Rep.*, 2011, **1**, 83.
63 E. Burstein, *Phys. Rev.*, 1954, **93**, 632–633.
64 T. S. Moss, *Proc. Phys. Soc., London, Sect. B*, 1954, **67**, 775–782.
65 S. Kazaoui, in *AIP Conference Proceedings*, AIP, 2000, vol. 544, pp. 400–403.
66 M. V. Kharlamova, L. V. Yashina, A. A. Volykhov, J. J. Niu, V. S. Neudachina, M. M. Brzhezinskaya, T. S. Zyubina, A. I. Belogorokhov and A. A. Eliseev, *Eur. Phys. J. B*, 2012, **85**, 1–8.
67 H. Farhat, H. Son, G. G. Samsonidze, S. Reich, M. S. Dresselhaus and J. Kong, *Phys. Rev. Lett.*, 2007, **99**, 1–4.
68 K. Sasaki, H. Farhat, R. Saito and M. S. Dresselhaus, *Phys. E*, 2010, **42**, 2005–2015.
69 A. M. Rao, P. C. Eklund, S. Bandow, A. Thess and R. E. Smalley, *Nature*, 1997, **388**, 257–259.
70 S. Cambré, B. Schoeters, S. Luyckx, E. Goovaerts and W. Wenseleers, *Phys. Rev. Lett.*, 2010, **104**, 1–4.
71 K. Sreelatha and P. Predeep, *IOP Conf. Ser. Mater. Sci. Eng.*, 2015, **73**, 012012.
72 R. T. P. Sant'Anna, C. M. P. Santos, G. P. Silva, R. J. R. Ferreira, A. P. Oliveira, C. E. S. Côrtes and R. B. Faria, *J. Braz. Chem. Soc.*, 2012, **23**, 1543–1550.
73 M. M. Alam, F. O. Lucas, D. Danieluk, A. L. Bradley, K. V. Rajani, S. Daniels and P. J. McNally, *J. Phys. D: Appl. Phys.*, 2009, **42**, 225307.
74 L. O'Reilly, O. F. Lucas, P. J. McNally, A. Reader, G. Natarajan, S. Daniels, D. C. Cameron, A. Mitra, M. Martinez-Rosas and A. L. Bradley, *J. Appl. Phys.*, 2005, **98**, 113512.
75 B. P. Gorshunov, E. S. Zhukova, J. S. Starovatykh, M. A. Belyanchikov, A. K. Grebenko, A. V. Bubis, V. I. Tsebro, A. A. Tonkikh, D. V. Rybkovskiy, A. G. Nasibulin, E. I. Kauppinen and E. D. Obraztsova, *Carbon*, 2018, **126**, 544–551.
76 Z. Li, F. Qin, T. Liu, R. Ge, W. Meng, J. Tong, S. Xiong and Y. Zhou, *Org. Electron.*, 2015, **21**, 144–148.

 

77 Z. Banyamin, P. Kelly, G. West and J. Boardman, *Coatings*, 2014, **4**, 732–746.
78 M. Yarali, J. Hao, M. Khodadadi, H. Brahmi, S. Chen, V. G. Hadjiev, Y. J. Jung and A. Mavrokefalos, *RSC Adv.*, 2017, **7**, 14078–14087.
79 K. Bradley, S.-H. Jhi, P. G. Collins, J. Hone, M. L. Cohen, S. G. Louie and A. Zettl, *Phys. Rev. Lett.*, 2000, **85**, 4361–4364.
80 B. Kaiser, Y. W. Park, G. T. Kim, E. S. Choi, G. Düsberg and S. Roth, *Synth. Met.*, 1999, **103**, 2547–2550.
81 A. Kaiser, G. Düsberg and S. Roth, *Phys. Rev. B: Condens. Matter Mater. Phys.*, 1998, **57**, 1418–1421.
82 A. B. Kaiser, *Adv. Mater.*, 2001, **13**, 927–941.
83 G. Fu, H. Zheng, Y. He, W. Li, X. Lü and H. He, *J. Mater. Chem. C*, 2018, **6**, 10589–10596.
84 L. Yan, X. Shen, Y. Zhang, T. Zhang, X. Zhang, Y. Feng, J. Yin, J. Zhao and W. W. Yu, *RSC Adv.*, 2015, **5**, 54109–54114.
85 B. Li, G. Fu, J. Guan, Y. He, L. Liu, K. Zhang, J. Guo, W. Feng and X. Lü, *J. Lumin.*, 2018, **204**, 30–35.
86 S. Suchalkin, Y. Lin, L. Shterengas, G. Kipshidze, D. Westerfeld and G. Belenky, *Superlattices Microstruct.*, 2016, **100**, 142–147.
87 Y. Muramoto, M. Kimura and S. Nouda, *Semicond. Sci. Technol.*, 2014, **29**, 084004.
88 Y. Li, W. Wang, L. Huang, Y. Zheng, X. Li, X. Tang, W. Xie, X. Chen and G. Li, *J. Mater. Chem. C*, 2018, **6**, 11255–11260.
89 P. Laiho, K. Mustonen, Y. Ohno, S. Maruyama and E. I. Kauppinen, *ACS Appl. Mater. Interfaces*, 2017, **9**, 20738–20747.